Practical Dosimetric Equivalence of New RTsafe 3D Printing Technologies

A TPS-based comparison of patient-specific cranial SRS phantoms produced using three different 3D Printers

1. Background

RTsafe previously characterized a patient-specific 3D-printed cranial phantom workflow in the peer-reviewed study by Makris et al. The reference method used a patient planning CT, segmented the external contour and bone structures, printed an anthropomorphic head phantom with high-density bone-mimicking material, filled the head volume with water and incorporated a film-dosimetry insert. The study evaluated the phantom as a patient-equivalent object by combining image fusion, Hounsfield-unit (HUs) and density checks, dose isoline comparisons, DVH and dose-volume metrics, 3D gamma-index analysis and film dosimetry. The reported computational gamma-index passing rates were better than 97% at 1%/1 mm, and absolute film-dosimetry gamma passing rates were above 90%. These results established the Zprinter 460 printing workflow as a credible transfer standard for cranial SRS quality assurance [1].

The present work extends that logic to technology change control. RTsafe has acquired two new 3D printers, Stratasys Objet500 Connex3 and Stratasys J5 Digital Anatomy. The practical question is whether phantoms manufactured with the new printers behave equivalently to those produced with the Zprinter 460 printer when the same treatment-planning-system (TPS) workflow is followed. This is the appropriate framing for product continuity: if the new printers reproduce the clinically relevant dose geometry and attenuation behavior of the Zprinter 460 printer within accepted QA tolerances, they can be considered practically equivalent for the intended phantom-manufacturing use.

2. Materials and method

Three identical 3D-printed anthropomorphic phantoms were produced using the three available 3D-printers: (i) Zprinter 460, (ii) Stratasys Object500 Connex3 and (iii) Stratasys J5 Digital Anatomy. Three CT acquisitions were performed for each phantom. A radiotherapy treatment plan was generated on each obtained CT dataset. The dose distribution calculated on the CT datasets of the Zprinter 460 phantom was defined as the reference distribution (REF). The dose distributions calculated for the Stratasys Object500 Connex3 phantom and Stratasys J5 Digital Anatomy phantoms were defined as Eval1 and Eval2, respectively. Eval1 and Eval2 were quantitatively and qualitatively compared with REF to investigate inter-printer dosimetric equivalence and identify potential manufacturing related effects on calculated dose deposition. The image set included axial, coronal and sagittal CT views with isodose overlays,one-dimensional dose profiles and absolute gamma-index maps. [2].

The dosimetric equivalence was assessed according to three predefined criteria. First, the spatial concordance of the Eval1 and Eval2 isodose lines with those of REF was examined, with particular emphasis on prescription dose regions, high dose gradient interfaces, and areas adjacent to tissue-equivalent material boundaries. Second, the agreement among the REF, Eval1, Eval2 dose profiles was evaluated in terms of profile shape, dose magnitude, field-edge position, and dose-gradient characteristics along the selected axial, coronal and sagittal directions. Third, the spatial distribution and magnitude of gamma-index deviations were assessed to determine whether discrepancies were low-amplitude and spatially confined or whether they formed coherent patterns indicative of systematic printer-dependent effects, such as differences in CT-number-to-density representation, material composition, dimensional accuracy, geometric scaling, or image registration.

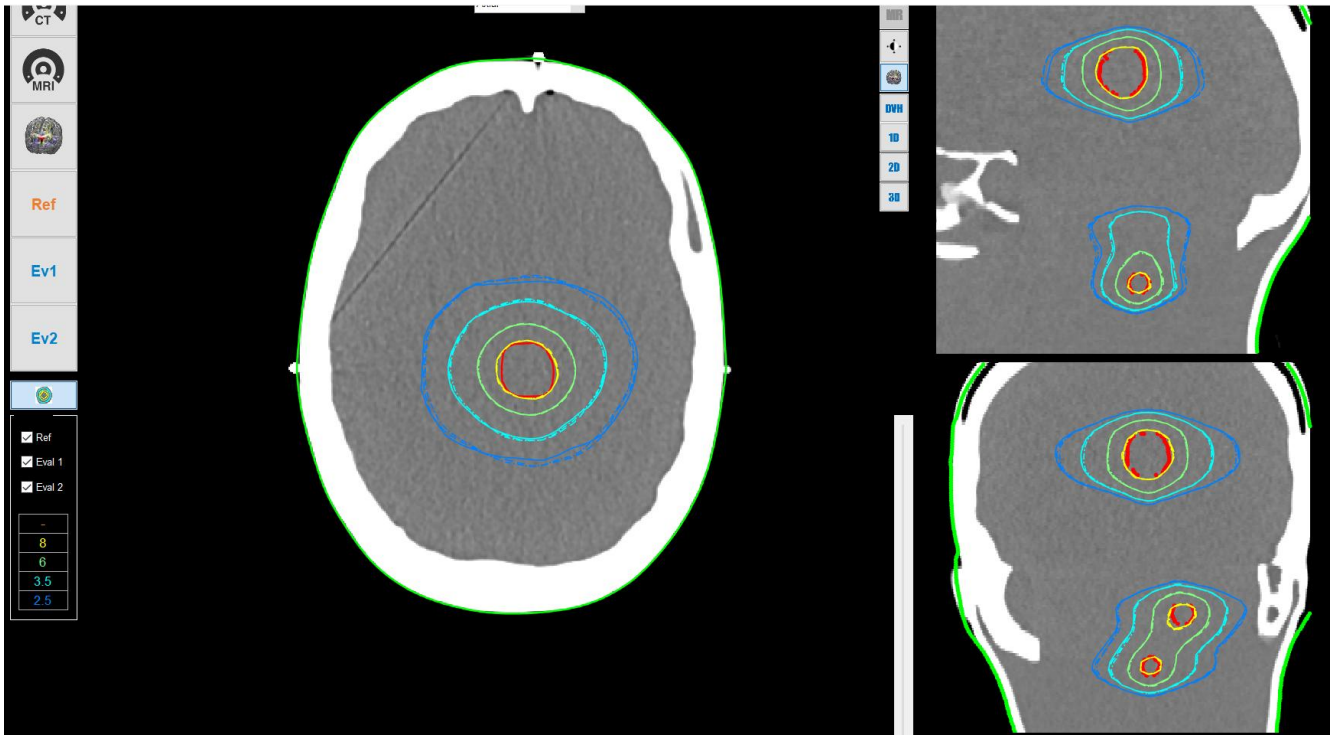

Figure 1. Multi-planar CT views with REF, Eval1 and Eval2 isodose overlays. The axial, sagittal and coronal panels show closely co-localized high- and intermediate-dose isolines.

3. Results

Visual comparison of the isodose distributions demonstrated a high degree of spatial agreement among REF, Eval1 and Eval2 (Figure 1). In the axial plane, the dose distributions surrounding the cranial target exhibited comparable geometry, with no evident expansion, contraction, or lateral displacement of the 8, 6, 3, 2 or 1.5 Gy isolines (Figure 2). Minor contour variations were observed predominantly in the low-dose region and at steep dose-gradient interfaces. However, these deviations were limited in spatial extent and did not exhibit a consistent printer-specific pattern. In particular, no systematic displacement or dimensional change was observed across multiple anatomical planes. Such a coherent pattern would be expected in the presence of printer-dependent differences in phantom geometry, material density, CT-number representation, or spatial registration.

In addition, the axial dose profiles showed agreement among REF, Eval1, and Eval2 along both the horizontal and vertical evaluation paths (Figures 3-4). Within the high-dose region, the profiles demonstrated comparable dose magnitudes and plateau widths. The positions and slopes of the field edges and penumbral regions were also closely aligned, indicating preservation of spatial registration, calculated attenuation, and dose-gradient characteristics across the three phantom types. Small deviations were observed within the low-dose tails of the profiles. These differences were visually limited and did not demonstrate a consistent positive or negative dose bias for either Eval1 or Eval2. The agreement across the complete profiles, including both low-gradient and high-gradient regions, provides evidence that the evaluated printing systems reproduced the spatial and dosimetric characteristics of the REF phantom more comprehensively than could be established through isolated point-dose comparisons alone.

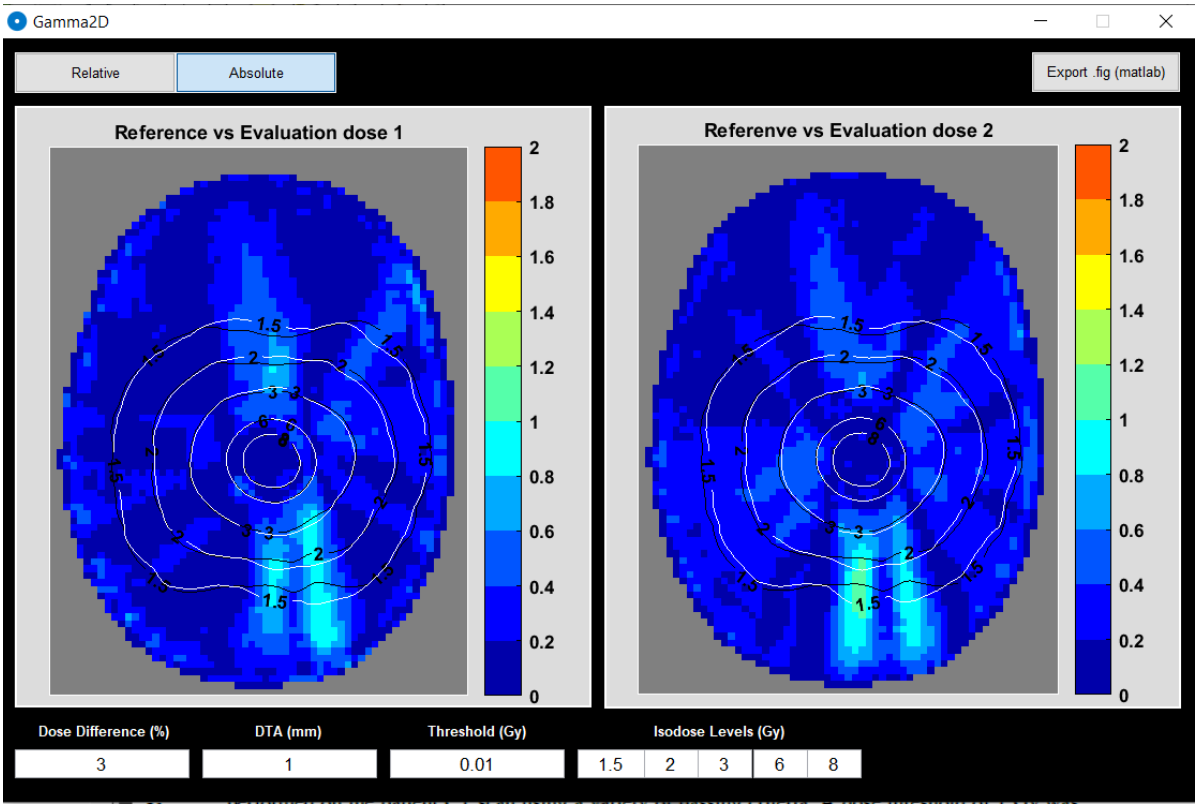

Figure 2. Axial absolute gamma-index maps for REF versus Eval1 and REF versus Eval2 using GI criteria of 3%/1 mm and 0.01 Gy threshold. The maps are predominantly low gamma values with localized higher values in steep-gradient and lower-dose regions.

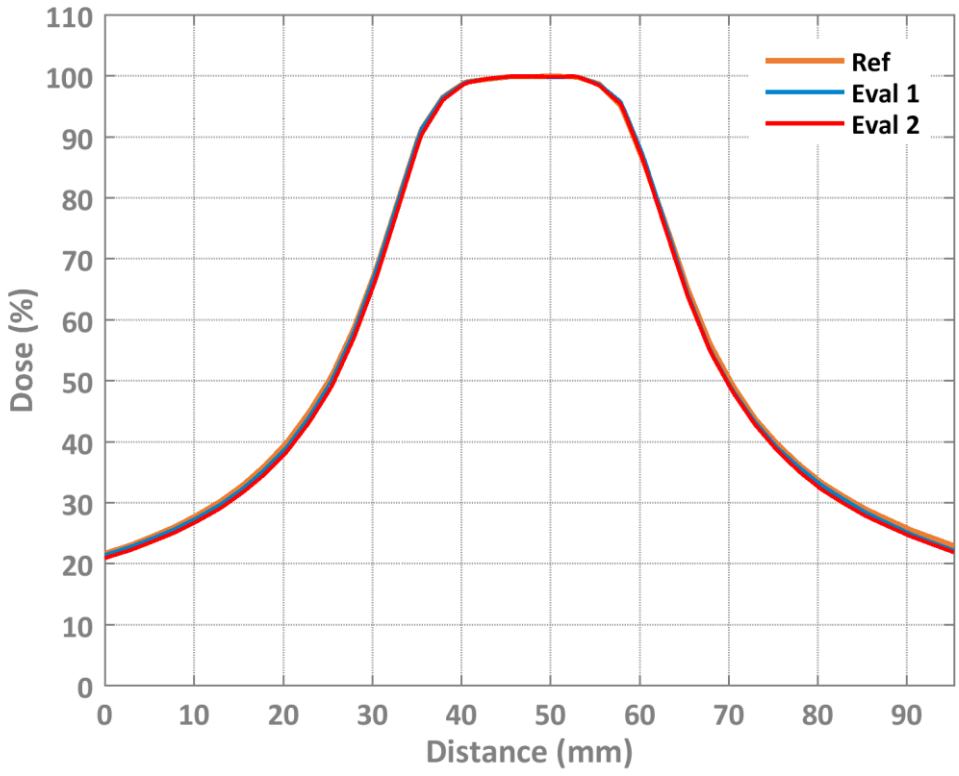

Figure 3. Axial horizontal dose profile. REF, Eval1 and Eval2 profiles are visually superimposed across the high-dose plateau and fall-off.

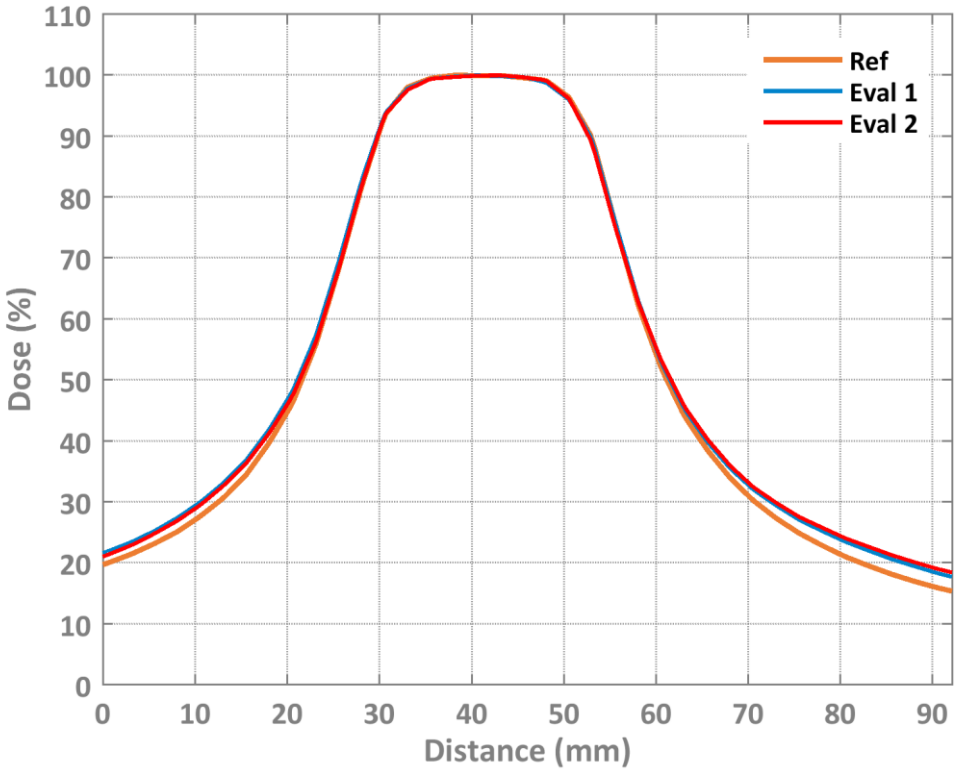

Figure 4. Axial vertical dose profile. The three profiles track each other through the target, shoulders and low-dose tails.

The coronal-plane analysis enabled assessment of dosimetric agreement over an extended superior–inferior distance and across two spatially separated high-dose regions. The vertical dose profiles (Figure 6) demonstrated comparable peak amplitudes, peak widths, and dose fall-off characteristics for both the superior and inferior irradiated regions. No systematic displacement of either dose peak was observed for Eval1 or Eval2 relative to REF.

Consistent with the axial findings, the coronal gamma-index maps showed predominantly low gamma-index values, with only localized regions of increased values (Figure 5). Neither Eval1 nor Eval2 exhibited an extensive or coherent failure pattern. Overall, the combined isodose, dose-profile, and gamma-index analyses showed no visually identifiable systematic printer-dependent differences relative to the REF dose distribution.

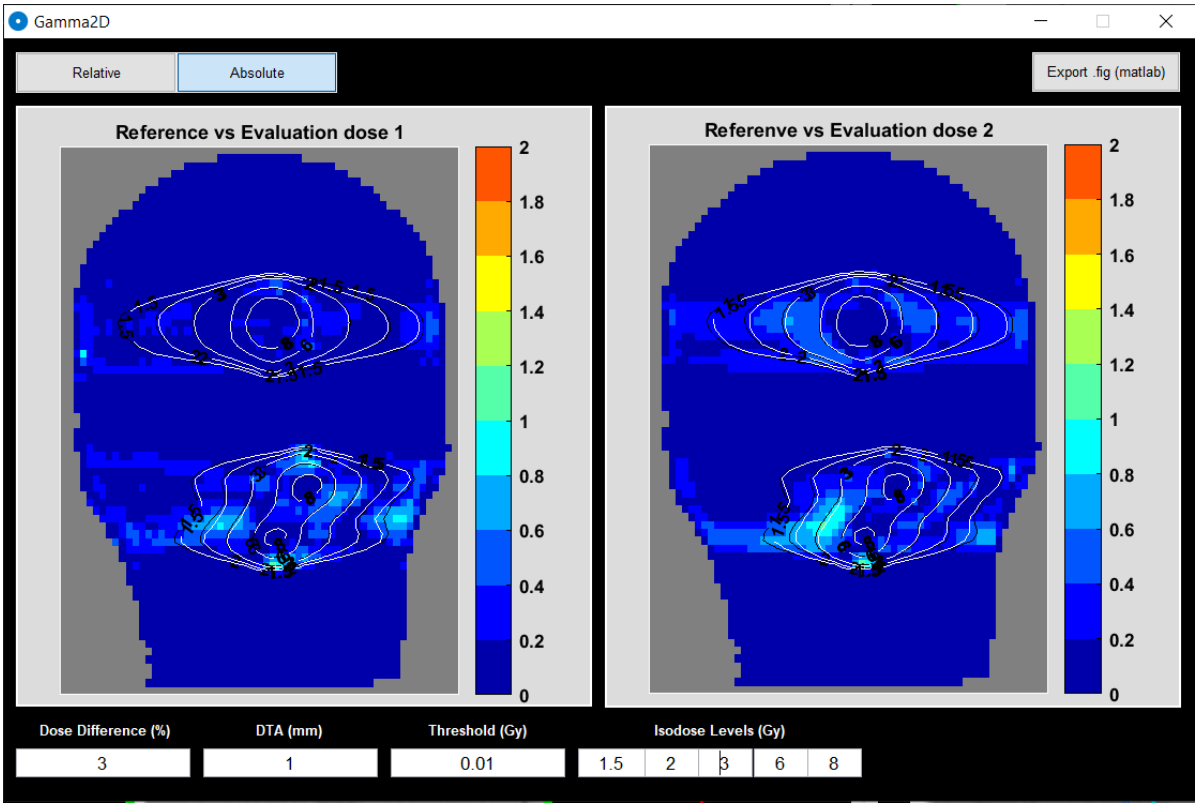

Figure 5. Coronal absolute gamma-index maps. Agreement is maintained for both the superior cranial dose region and inferior structure, with localized differences remaining comparable for Eval1 and Eval2.

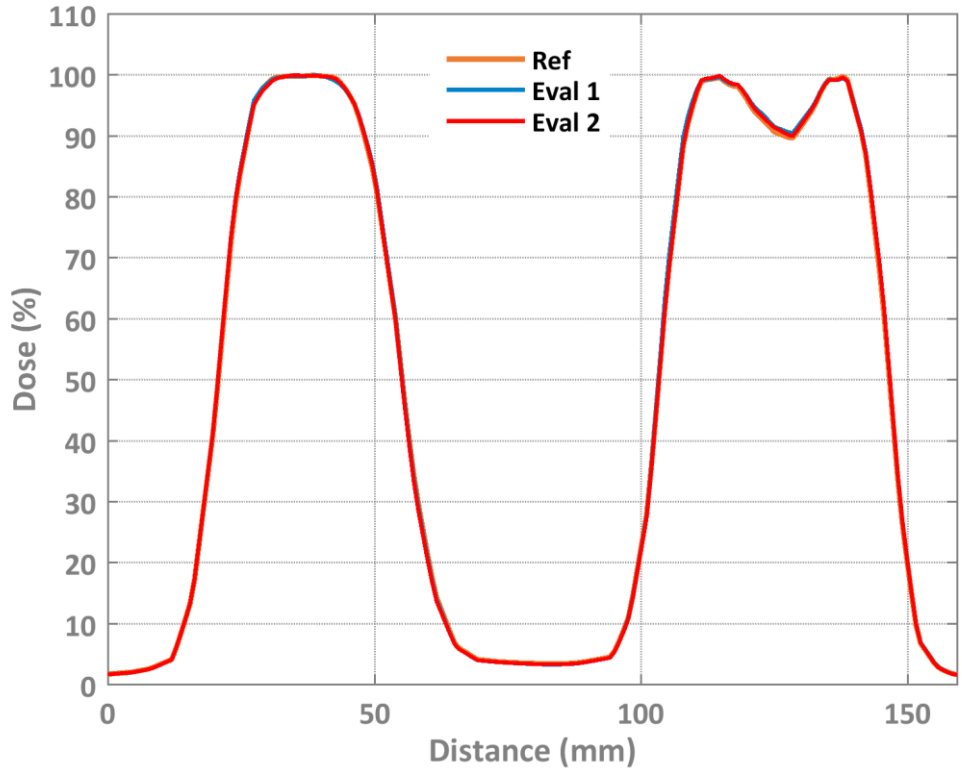

Figure 6. Coronal vertical dose profile. The two separated high-dose regions show matched peak level, width and fall-off for REF, Eval1 and Eval2.

A similar pattern of dosimetric agreement was observed in the sagittal plane. The REF, Eval1, and Eval2 isodose distributions exhibited similar spatial extent, contour morphology, and dose fall-off across the anterior–posterior and superior–inferior directions. The corresponding sagittal dose profiles (Figure 8) showed close agreement in peak dose, profile width, field-edge position, and penumbral gradient, with only minor localized deviations in the low-dose regions.

The sagittal gamma-index maps (Figure 7) were likewise dominated by low gamma-index values, while regions of increased values remained spatially confined and were primarily located at steep dose-gradient interfaces. No coherent pattern of elevated gamma-index values, systematic target displacement, or deformation of the dose distribution was identified for either Eval1 or Eval2. These findings are consistent with the axial and coronal analyses and further support the absence of a systematic printer-dependent effect on the calculated dose distribution.

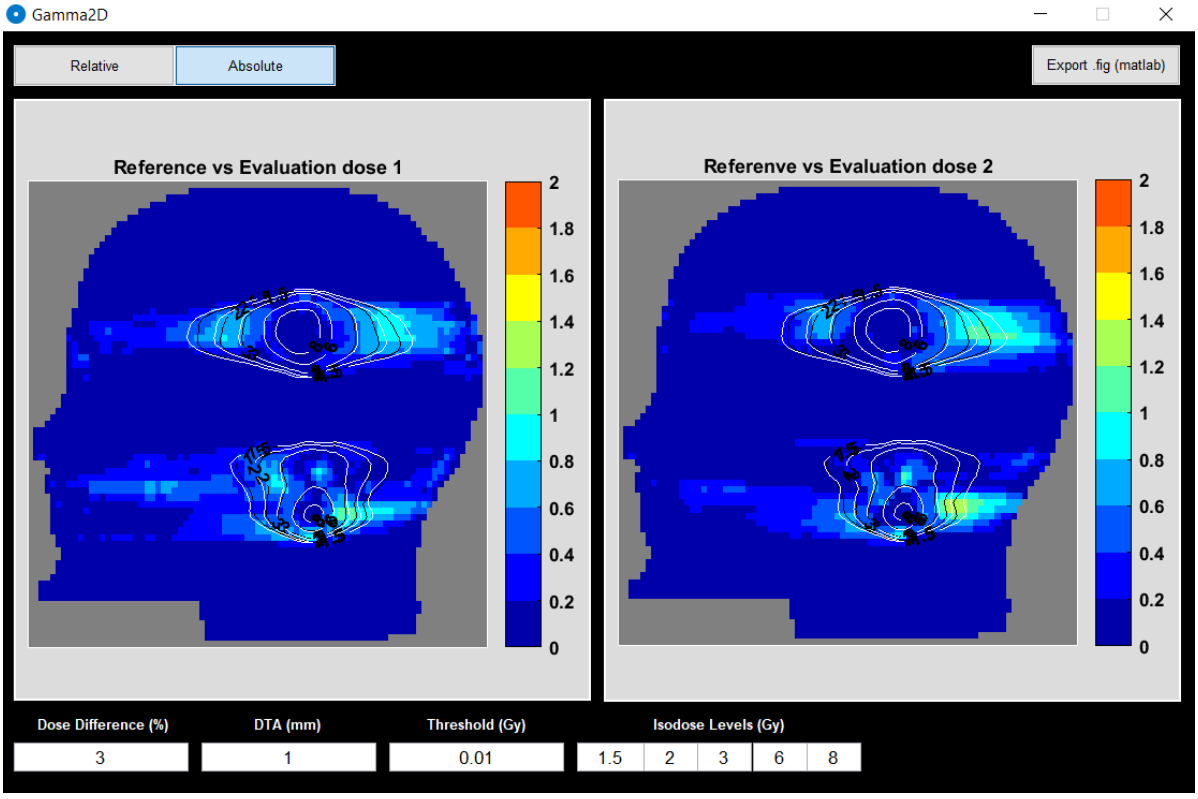

Figure 7. Sagittal gamma-index maps. Similar low-index distributions are observed for both evaluated printers.

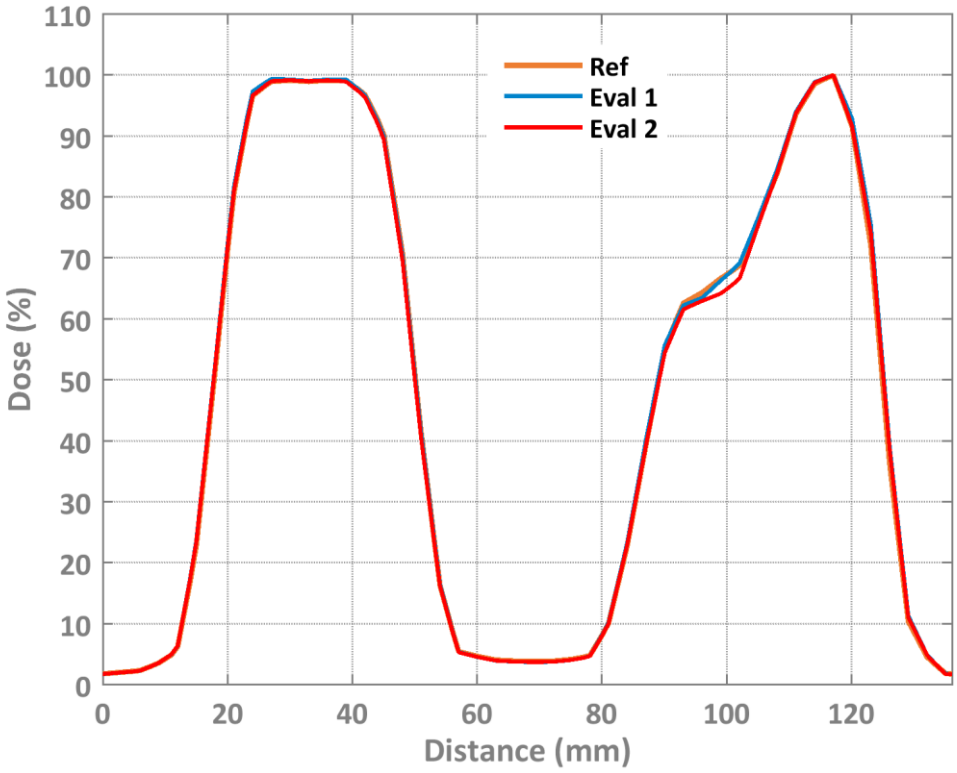

Figure 8. Sagittal vertical dose profile. The REF, Eval1 and Eval2 curves remain matched across the cranial dose peak, valley and inferior dose peak.

4. Interpretation: practical equivalence to the REF printer

The data support a practical equivalence statement because the same conclusion is reached through independent assesments of the dose distribution. Isodose overlays show spatial coincidence; one-dimensional profiles show agreement in peak dose, plateau shape and penumbra; and absolute gamma maps show low, localized disagreement rather than a systematic printer-dependent effect. This combination mirrors the logic of the Makris et al. characterization paper: anatomical and computational agreemenshould be demonstrated in the dose quantities that matter for stereotactic QA, not inferred solely from printer specifications.

Using the REF printer as a transfer standard is scientifically defensible because REF has already been characterized in the clinical phantom workflow. Eval1 and Eval2 are therefore required to reproduce the REF behavior under the same TPS calculation conditions. The supplied evidence indicates that they do. In practical terms, the new printers are considered interchangeable with REF for the evaluated cranial SRS phantom workflow, provided that routine production QA confirms geometry, CT number/density consistency and absence of printing artifacts on each released phantom.

5. Evidence summary and recommended acceptance language

Evidence stream	Observation in supplied images	Equivalence implication
Isodose overlays	REF, Eval1 and Eval2 isolines are closely co-localized in axial, coronal and sagittal views.	No visible systematic geometric or attenuation-related dose shift.
Dose profiles	The three profiles are visually superimposed through peaks, shoulders, penumbra and low-dose regions.	Peak level, field width and fall-off are preserved by the new printers.
Absolute gamma maps	Maps are dominated by low gamma values, with localized higher values that are similar for Eval1 and Eval2.	Residual differences are local and not printer-specific.
Multi-plane consistency	Agreement is maintained across orthogonal planes and separated dose regions.	Equivalence is not limited to a single slice or single line.

Based on TPS-calculated dose distributions and the available image exports, the Eval1 and Eval2 3D printing technologies demonstrated practical dosimetric equivalence to the characterized REF printer for the evaluated patient-specific cranial SRS phantom workflow. This conclusion was supported by the spatial co-registration of the isodose distributions, close agreement of the one-dimensional dose profiles, and comparable absolute gamma-index distributions in the axial, coronal, and sagittal planes. No systematic printer-dependent deviation in dose magnitude, dose-gradient position, high-dose-region geometry, or spatial registration was identified within the scope of the present evaluation.

Conclusion

The REF printing system established the RTsafe patient-specific cranial stereotactic radiosurgery phantom workflow through comprehensive imaging, dosimetric, and measurement-based characterization. Within the scope of the present treatment-planning-system evaluation, the Eval1 and Eval2 additive-manufacturing systems reproduced the clinically relevant dosimetric characteristics of the REF phantom.

Consistent agreement was observed across the axial, coronal, and sagittal planes, including spatially co-registered isodose distributions, preservation of one-dimensional dose-profile shape and position, and comparable absolute gamma-index patterns. No systematic printer-dependent differences were identified in dose magnitude, high-dose-region geometry, penumbral characteristics, dose-gradient location, or spatial registration. The residual discrepancies were localized predominantly to low-dose and high-gradient regions and did not exhibit coherent patterns suggestive of systematic differences in phantom geometry or radiological properties.

These findings support the practical dosimetric equivalence of the Eval1 and Eval2 printing technologies to the characterized REF system for the evaluated patient-specific cranial SRS phantom application. Subject to routine manufacturing quality assurance, verification of dimensional and radiological consistency, and documentation of quantitative gamma-analysis pass rates using predefined acceptance criteria, Eval1 and Eval2 may be implemented as equivalent additive-manufacturing technologies within the established RTsafe cranial phantom workflow.

References

Makris DN, Pappas EP, Zoros E, Papanikolaou N, Saenz DL, Kalaitzakis G, Zourari K, Efstathopoulos E, Maris TG, Pappas E. Characterization of a novel 3D printed patient specific phantom for quality assurance in cranial stereotactic radiosurgery applications. Physics in Medicine and Biology. 2019;64(10):105009. doi:10.1088/1361-6560/ab1758.

Low DA, Harms WB, Mutic S, Purdy JA. A technique for the quantitative evaluation of dose distributions. Medical Physics. 1998;25(5):656-661. doi:10.1118/1.598248.